LBL-31572
UC-404

Lawrence Berkeley Laboratory

UNIVERSITY OF CALIFORNIA

Materials Sciences Division

A Coarsening Model for Coherent Precipitates

M.T. McCormack
(Ph.D. Thesis)

December 1991

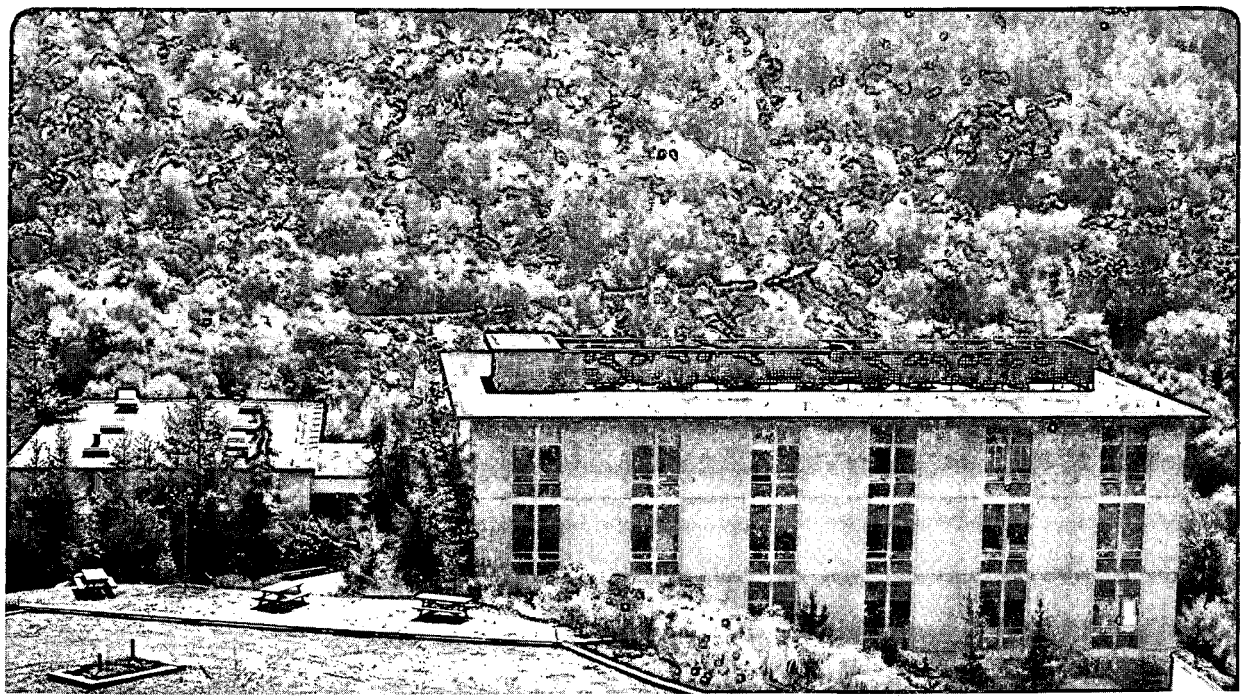

Prepared for the U.S. Department of Energy under Contract Number DE-AC03-76SF00098

DISCLAIMER

This document was prepared as an account of work sponsored by the United States Government. While this document is believed to contain correct information, neither the United States Government nor any agency thereof, nor the Regents of the University of California, nor any of their employees, makes any warranty, express or implied, or assumes any legal responsibility for the accuracy, completeness, or usefulness of any information, apparatus, product, or process disclosed, or represents that its use would not infringe privately owned rights. Reference herein to any specific commercial product, process, or service by its trade name, trademark, manufacturer, or otherwise, does not necessarily constitute or imply its endorsement, recommendation, or favoring by the United States Government or any agency thereof, or the Regents of the University of California. The views and opinions of authors expressed herein do not necessarily state or reflect those of the United States Government or any agency thereof or the Regents of the University of California.

LBL 31572

A Coarsening Model for Coherent Precipitates

Mark Thomas McCormack

Ph.D. Dissertation

Department of Materials Science and Mineral Engineering
University of California
and
Center for Advanced Materials
Materials Sciences Division
Lawrence Berkeley Laboratory
University of California
Berkeley, CA 94720

December 1991

This work was supported by the Director, Office of Energy Research, Office of Basic Energy Science, Materials Science Division of the U.S. Department of Energy under Contract No. DE-AC03-76F00098

A Coarsening Model for Coherent Precipitates

Copyright © 1991

Mark Thomas McCormack

Ph.D. Thesis

The United States Department of Energy has the right to use this thesis for any purpose whatsoever including the right to reproduce all or any part thereof

A Coarsening Model for Coherent Precipitates

by

Mark Thomas McCormack

Abstract

The morphological evolution of coherent inclusions in elastic media is studied in two-dimensions. The inclusions are simple dilations with isotropic surface energy in a system with homogeneous elastic constants of negative anisotropy. The equilibrium sizes at which a circular inclusion transforms to a rectangle or square, and at which a square splits into a doublet or quartet of separated inclusions are computed analytically. A finite-element model is then constructed to simulate the evolution of an arbitrary distribution of inclusions along the minimum-energy path. In the model, the circle evolves into a square, which splits into a doublet by hollowing from its center, or, if this is forbidden, by drawing in a perturbation on its surface. The sizes at which shapes spontaneously transform are compared to the equilibrium values. Finally, the simulation is used to study the evolution of a random distribution of inclusions. The first metastable state assumed by the distribution depends on the elastic interaction, surface energy and areal fraction of the inclusion phase through a single dimensionless parameter that groups these three effects. The results are compared to prior theoretical and experimental work on coarsening patterns in three dimensions.

ACKNOWLEDGEMENTS

Words do no justice in describing the deep appreciation and respect I hold for my research advisor, Professor J.W. Morris, Jr. Thanks, Bill. You are our surrogate Daddy; you mean so much to so many.

Speaking of family, THANK YOU Mom and Dad for supporting me all these years. I'm still trying hard. Nonetheless, as I write this, I'm still just a bum without a job -- I know, I KNOW! One day we'll laugh about it. Hope it's soon.

I'd like to thank Professor Armen G. Khachaturyan, now at Rutgers, for the opportunity I had to work with him. It was a most valuable experience. In addition, I'd like to thank Professors Ron Gronsky and Boris Rubinsky for taking the time from their busy schedules to read and approve my thesis.

I'd like to thank all my Morris Group colleagues, past and present, for everything.

Finally, I'd like to thank my fiancée, Ingrid Nilson. We wouldn't be together if I hadn't gone through this whole graduate school experience. Ingrid, you've made it all worthwhile. I'd do it all over again!

This work was supported by the Director, Office of Energy Research, Office of Basic Energy Sciences, Materials Sciences Division of the U.S. Department of Energy under Contract No. DE-AC03-76SF00098

TABLE OF CONTENTS

PAGE

I. INTRODUCTION 1

A. Coherent Precipitates Display Different Coarsening Behavior 1

B. Scope of Thesis 3

II. BACKGROUND 6

A. Dynamic Coarsening Models 6

i. Lifshitz-Slyozov-Wagner (LSW) Coarsening 6

ii. Modified LSW Analyses 9

iii. Statistical Methods 11

iv. Geometrically General Model 12

v. Dynamic Coarsening Models That Incorporate Elastic Effects 13

B. Energetic Coarsening Models 15

i. Energetic Monte Carlo Methods 15

ii. Energetically Deterministic Methods 16

III. ANALYTIC MODEL 17

A. The Elastic Energy 17

B. The Surface Energy 21

IV. EQUILIBRIUM SHAPES IN TWO DIMENSIONS....23

V. FINITE ELEMENT MODEL....28

A. The Elastic Energy....29

B. The Surface Energy....32

VI. SHAPE TRANSITIONS IN COMPUTER SIMULATION....35

A. Procedure....35

B. Evolution of an Initially Circular Inclusion....38

i. Circle to Square....38

ii. Square to Doublet....40

iii. Square to Quartet....42

C. Evolution of a Random Distribution of Inclusions....43

VII. DISCUSSION....45

A. Results of the Model....45

B. Limitations of the Model....47

VIII. REFERENCES....49

IX. FIGURES....53

I. Introduction

I.A. Coherent Precipitates Display Different Coarsening Behavior

Descriptions of microstructural stability are often based upon the equilibrium and stability of fluid systems. For example, the microstructures of multi-phase fluids are always unstable if the total interfacial free energy is not a minimum. This instability is evident in the common observation that a high density of small precipitates always tends to *coarsen*, or ripen, into a lower density of larger particles with a smaller total interfacial area. Such precipitate coarsening processes also take place in multi-phase solids, where they often produce an undesirable degradation of properties, e.g., a loss of mechanical strength.

The difference between droplets of a precipitate phase in fluids and precipitates in multi-phase solids can be categorized according to the *coherency* of the precipitate/matrix interface. Coherency refers to the continuity of the crystal lattice across the interface. Incoherent precipitates lack any such continuity, and therefore only hydrostatic stresses may be transmitted across the boundary. Since hydrostatic stresses are essentially pressures, incoherent precipitates can be expected to behave much in the same manner as minority phase droplets in fluid phase systems. Coherent precipitates, on the other hand, maintain full lattice continuity across the interface. This lattice continuity allows both shear and hydrostatic stresses to be transmitted across the particle boundary. Coherent precipitates in solids can therefore interact elastically with one another in a distinctly different manner than that which can be described in fluid systems.

For a distribution of precipitates in a fluid, the droplets are usually observed to coarsen as spheres with a mean droplet size increasing monotonically with time. In comparison, the coarsening of a distribution of coherent precipitates in a solid differs qualitatively from that observed when the precipitates are incoherent and have no elastic interaction with one another. A widely studied example is the coarsening of the cubic γ' precipitates in Ni-based alloys. When the precipitates are densely distributed, they interact and align with one another to create stable patterns that coarsen very slowly. When they are widely separated, they evolve from spheres to cubes to plates as they grow, and sometimes split spontaneously into parallel plates or octets of small cubes [1-8]. Such peculiar coarsening behavior is usually attributed to the effects of elastic strains generated in the coherent accommodation of the misfitting γ' phase.

I.B Scope of Thesis

Since precipitate coarsening can strongly influence the mechanical properties of materials, it is important that all aspects of coarsening be understood in order to reliably predict and control its extent. In this regard, it has been common modeling practice to assume the coarsening medium is a two-phase fluid. As reviewed by Voorhees [9], studying the coarsening of droplets in this manner is valuable in identifying the shortcomings encountered when extending the classic Lifshitz-Sloyzov-Wagner [10-12] analysis to systems containing finite fractions of the precipitate phase. Fluid phase descriptions, while sufficient to describe the coarsening behavior in many alloy systems, are incapable of predicting all the coarsening phenomena observed in solids containing a coherent precipitate phase. It is thus necessary to incorporate elastic effects into coarsening models in order to better understand the unusual coarsening behavior of coherent precipitates.

A complete theory of coarsening for coherent precipitates must consider both the elastic interactions that determine the relative elastic energy of the precipitate configuration and the diffusional processes that govern the rate at which the configuration evolves. Both the thermodynamic and kinetic elements of the theory are difficult to formulate. The elastic interaction that determines precipitate shape and alignment is due to the lattice mismatch between the precipitate and matrix phases, and is strongly affected by elastic anisotropy. The kinetics of the diffusional processes that govern growth are affected not only by the sizes and shapes of the particles, but also by the elastic fields in the matrix.

A number of investigations have studied aspects of the theory of coherent precipitate coarsening [13-41]. In particular, prior work by several authors has addressed the energetics of coherent precipitates in anisotropic media, exploiting techniques that permit an

exact calculation of the elastic energy of a homogeneous, anisotropic system that contains an arbitrary distribution of inclusions. The results of that work show that elastic anisotropy leads to the alignment of distributions of cubic or tetragonal precipitates [36-39], that a precipitate of cubic phase with an isotropic surface tension systematically evolves from a spherical to a cubic to a platelet shape as it grows in a homogeneous matrix [40], and that a coherent cube of cubic-phase material becomes sequentially metastable with respect to splitting into a parallel pair of platelets and an octet of small cubes as its size increases [41]. The results include most of the important morphological changes that have been observed in γ' precipitates.

The present work was undertaken in order to bridge the models that were employed in this previous work. In the computer simulation studies of precipitate alignment by Wen, et al. [36-39], the precipitate particles were assumed discrete and separate, and were constrained to remain so. Hence this work only suggests the coarsening patterns of a distribution of precipitates. In the studies of particle shapes by Khachaturyan, et al. [40-41] the preferred shapes were identified by comparing the elastic energies of a pre-selected set of candidate shapes. This method risks missing other shapes that may be preferred during coarsening, and calculates the equilibrium transitions, while actual transitions are more likely driven by morphological instabilities. In the present work we study the elastic energy of distributions of dilational inclusions in cubic matrix, and follow the evolution of shape and distribution as the energy decreases along the path of steepest descent.

For computational simplicity the calculations that are presented here are done in two dimensions. Both the analytic and experimental demonstrations of such important phenomena as the spontaneous splitting of cubic precipitates refer to three-dimensional particles. To establish contact between the two-dimensional case treated here and three-dimensional behavior, we must first calculate the equilibrium shapes of two-dimensional precipitates as a function of size.

We then develop a computer simulation model that treats a two-dimensional elastic solid as a periodic distribution of square, elementary particles that have a long-range elastic interaction with one another, supplemented by a near-neighbor interaction that simulates surface energy. A configuration of precipitate particles is introduced by imposing a given transformation strain on a selected set of these elementary particles. The configurational energy (elastic plus surface energy) is then computed, together with the change in energy that would be accomplished by small reconfigurations of the precipitate distribution. In this way we test the elastic stability of the distribution, and identify the sequence of morphological changes that occurs as an unstable configuration evolves along the path of steepest descent in the energy. Two basic problems are investigated: the change of an initially circular particle during growth and the evolution of an initially random distribution of small interacting inclusions.

The model developed here is limited in three ways to facilitate computation. First, as in prior work [36-41], we assume a linear elastic medium with homogeneous elastic constants. The assumption of elastic homogeneity allows use of the methods of Khachaturyan and Shatalov [42] to compute the elastic energy of an arbitrary distribution of elastic inclusions. Second, we assume that the system is two-dimensional and periodic. Third, we focus on the kinematics of coarsening and calculate the sequence of states assumed as the system evolves toward equilibrium along the path of steepest descent in the elastic energy. Other investigators [28-33] have made progress toward a kinetic analysis of the coarsening of elastic inclusions, but at considerable cost in computational effort. As we shall see, many of the interesting features of the process are clearly revealed in the simpler, kinematic treatment, including the splitting of monolithic inclusions and the geometric alignment of discrete particles.

II. Background

Incorporating elastic effects into coarsening models is a formidable task that requires a significant amount of idealization. In order to appreciate these difficulties, it is important to first understand the results developed from various fluid droplet analyses. Coarsening models have historically concentrated on dynamic models which are concerned with the rate at which coarsening events take place. Energetic models, on the other hand, are principally concerned with what coarsening events are possible. While these two modeling premises are different, it is important that they both be pursued so that the ramifications of idealization in different models can be recognized and contribute to the understanding of all coarsening phenomena.

II.A Dynamic Coarsening Models

Most dynamic coarsening models are based upon one of two approaches, the Lifshitz-Slyozov-Wagner [10-12] mean-field analysis or the Weins-Cahn [43] microscopic formulation.

II.A.i Lifshitz-Slyozov-Wagner (LSW) Coarsening

The foundations of coarsening theory were established independently by Lifshitz and Slyozov [2,4], and Wagner [3]. They required a very idealized system to satisfy three equations during the coarsening process:

a) a kinetic equation - the diffusive flux at an individual precipitate's surface is equated to the precipitate's growth rate;

b) a continuity equation - the distribution of precipitate sizes is continuous in time;

c) a mass conservation equation - the solutions to both the kinetic and continuity equations must conserve the total solute concentration.

The idealized system considered in the LSW analysis assumes that:

i) both the precipitate and matrix phases are isotropic fluids;

ii) precipitates are spherical in shape;

iii) precipitate positions are fixed in space;

iv) there exists a sufficient number of precipitates for the distribution of precipitate radii to be represented as a continuous function;

v) processes such as nucleation and precipitate coalescence are neglected;

vi) the composition at the surface of a precipitate is determined by the radius of the precipitate;

vii) the total volume of the system is infinite.

The results of their analysis show that after a sufficient amount of time, coarsening will proceed in a steady state manner such that the precipitate size distribution (referenced to the mean precipitate size) is stationary in time. This asymptotic distribution is independent of the initial distribution at the start of coarsening. The mean precipitate radius in this coarsening regime, $\bar{a}$, increases monotonically: $\bar{a} = kt^{1/3}$, with the growth factor, k, being a constant. It is important to recognize the consequences of assumption (vii), wherein the total volume is regarded as infinite. In a finite volume the process is, of course, complete after a finite time, when the precipitates have coarsened into a single mass.

II. A. ii Modified LSW Analyses

The LSW analysis provides a remarkably successful description for the majority of coarsening observations, especially when one considers the restrictive set of assumptions that it employs. Real systems, however, tend to exhibit broader and more symmetric steady-state size distributions than those predicted by LSW. In addition, while the mean precipitate size is usually observed to coarsen at the predicted $t^{1/3}$ rate, the growth factor, k, is rarely found to be that predicted by LSW. In order to account for these discrepancies, critiques of the LSW analysis point out that assumption (vi) represents the situation in which a precipitate's coarsening rate is independent of its surroundings. This means a particle whose nearest neighbors are larger than itself will coarsen at exactly the same rate as if it were surrounded by precipitates that were of a smaller radius. This is only true in the limit of zero volume fraction, where precipitates are infinitely separated. Several investigations have been made to incorporate volume fraction effects into the LSW formalism.

Ardell [44] presented the first finite volume fraction modification to the LSW analysis. Assuming that a random spatial arrangement of different sized precipitates can be related through a mean free diffusion path which is a function of volume fraction, Ardell expressed the kinetic equation as a function of volume fraction and repeated the LSW analysis. The result showed that as volume fraction increases, the predicted growth rate factor increases and the theoretical size distribution broadens. The coarsening rate was found proportional to $t^{1/3}$ at all volume fractions, and the modifications include the LSW results in the zero volume fraction limit.

Davies, Nash and Stevens (DNS) modified the LSW analysis by relaxing assumption (v) as a function of volume fraction by altering the continuity equation to include the effect of direct contact, or welding, between growing precipitates [45]. Davies, et al. showed that the effect of such precipitate encounters is to increase the growth factor of the LSW analysis by a factor of approximately three, and to alter the shape of the steady-state distribution so that it broadens and becomes increasingly symmetric with increasing volume fractions. The $t^{1/3}$ coarsening dependence is unaffected by encounters and the results reduce to those of LSW at zero volume fraction.

Brailsford and Wynblatt* (BW) develop a different kinetic equation that assumes the growth rate of a precipitate of one size class is a function of both the entire particle size distribution and the prevailing concentration gradient around the particle [46]. Employing methods similar to LSW for the continuity of the size distribution, the results show the growth rate to be less sensitive to volume fraction than Ardell's theory, but more sensitive than found in the DNS encounter theory. The broadening of the steady-state size distribution is less than that found by Ardell and less than that found by DNS. These results also reduce to those of LSW at zero volume fraction. The predictions of DNS and BW provide the most reasonable agreement with most experimental data.

II. A. iii Statistical Methods

Since the phenomenological approach used in the LSW analysis is unsatisfying to many researchers, there has recently been great interest in using various statistical approaches to overcome the zero volume fraction assumption of the LSW theory. These statistical methods begin with a system of growth equations for precipitates that are similar in form to those first proposed by Weins and Cahn [43]. These coupled equations describe the radial growth of each precipitate and take into account the long-range interaction of the other precipitates which arise from the steady-state solution of the local concentration field. This entire system of equations is necessary in order to satisfy solute conservation. When emission or absorption of solute from growing or dissolving precipitates is modeled by placing point sources or sinks at the center of immobile spherical precipitates, the model is called a monopole approximation. When points along a precipitate's surface can serve as poles of different strength, it is called a multipole model. The strength of a pole is related to its curvature and growth rate. Solving the entire system of coupled equations becomes computationally difficult with even a relatively small number of poles. The goal of statistical analyses is to calculate statistically averaged pole strengths as a function of volume fraction.

As reviewed by Voorhees [9] and Gunton [47] , all early monopole models were based upon the equations of Weins and Cahn, but employed different statistical averaging schemes and arrived at different quantitative results. More recent studies [30-31,48-51] have modified the equations of Weins and Cahn in order to investigate spatial correlations within the statistical analyses and to reveal various other inadequacies of the earlier

monopole studies. Experimental data is, however, insufficient to support the claims of any of these models.

Multipole analyses [50-51] permit the study of mobile nonspherical precipitates, but these studies are computationally enormous, even when statistical averaging is employed. While these studies have proved successful in displaying motion and morphological changes of initially spherical precipitates upon coarsening, it is currently impractical to study a system's coarsening behavior using such models.

II.A.iv Geometrically General Model

Recently, DeHoff (52) has criticized previous coarsening theory and asserted that any coarsening theory that reduces to the mean field LSW result in the sparse sphere distribution limit (as all the previously dicussed models do) is inherently flawed. In DeHoff's model, *communicating neighbor* surface elements and local diffusion length scales are incorpoated into interparticle interactions. The geometrically general kinematic equations derived from these considerations yield results that sharply contrast LSW behavior in the low volume fraction limit. At present, there has been no subsequent work to substantiate DeHoff's claims.

II. A. v Dynamic Coarsening Models that Incorporate Elastic Effects.

Elastic effects have been introduced into dynamic coarsening models at both the many-body and two-body descriptive levels. Enomoto and Kawasaki [30-31] have, at present, provided the only many-body model incorporating an elastic energy interaction field. They consider a distribution of immobile elastically interacting spheres and couple an elastic contribution to the system of growth equations put forth by Weins and Cahn [43]. The elastic interaction field is that derived by Eshelby [1,53] : it assumes both an isotropic media and spherical inclusions. The inclusions are characterized by their dilational misfit and different elastic constants. Their analysis predicts that when the shear modulus of the precipitates is greater than that in the matrix phase, an inverse coarsening process occurs whereby smaller precipitates grow at the expense of the larger ones. This process slows the coarsening kinetics in their model at intermediate precipitate sizes, as has been observed in Ni-Al systems [5]. In contrast, when the precipitate phase has a relatively smaller shear modulus, they predict the coarsening kinetics to increase from the classic LSW $t^{1/3}$ dependence to a $t^{1/2}$ growth law. In addition, their steady-state precipitate size distributions display volume fraction dependencies similar to those experimentally observed in precipitates with higher relative shear moduli, such as Ni-Al, and those with lower relative shear moduli, such as Al-Zn [54]. However, neither monotonic growth of smaller precipitates at the expense of larger ones, nor the crossover to the higher $t^{1/2}$ growth law, has been experimentally observed. The statistical mechanics methodology of Enomoto and Kawasaki is quite complicated: revealing aspects concerning the foundations and justifications of their perturbative expansion technique are discussed by Gunton [47], Voorhees [9] , Beenakker [48], Marder [49] and Kawasaki [50-51].

Johnson, Voorhees and coworkers [22,24,27-29] are principally responsible for the present understanding of elastic effects in the dynamics of coarsening at the local level. They have investigated the two-body problem with coupled elastic and diffusion fields for dilational misfitting spherical inclusions, and have examined the influence of elastic isotropy and anisotropy upon precipitate orientations, spacings, and sizes on growth rates during coarsening. Their analysis permitted inclusions to be mobile, and it was found that a precipitate's center of mass can translate during coarsening. The two-body model predicts the same inverse coarsening as Enomoto and Kawasaki although, in contrast to Enomoto and Kawasaki, the inverse coarsening predicted in the isotropic case occurs for inclusions with relatively lower shear moduli at certain precipitate sizes and spacings [28]. In addition, the two-body simulation predicts inverse coarsening events in elastically anisotropic media regardless of any inhomogeneities between the elastic constants of the precipitate and matrix [29]. Since arbitrary geometries are difficult to employ in this two-body analysis, the model does not enable the prediction of either elastically induced shape changes, or the inverse coarsening process whereby large precipitates subdivide into a number of smaller ones.

II.B Energetic Coarsening Models

II.B.i Energetic Monte Carlo Methods

Monte Carlo methods have recently been utilized to simulate elastic effects in the coarsening of coherent precipitates. Gayda and Srolovitz [32] used a finite element formulation in order to consider short range elastic interactions between misfitting elements and used a Monte Carlo scheme to rearrange particles as to minimize their total energy. Lee [33] considered tetragonally misfitting elementary particles that interact at long range in an elastically isotropic medium, and used Monte Carlo methods to examine the dynamics of coarsening in his system. Monte Carlo simulations, such as these, have the distinct advantages: the method not only directly models a physical evolution process, but it also yields a rate for the process. Nevertheless, the method also carries interpretive difficulties. It requires one to treat an elastic particle as if it had a great deal of mobility in the matrix. In addition, treating elastic particles in the same manner as mobile atoms usually yields time snapshots of the process that are blurred from the random nature of the simulation. For example, grid regions of condensed particles often appear surrounded by a diffuse vapor of elastic particles. This is to be expected from Monte Carlo techniques, as they are essentially averaging techniques.

II.B.ii. Energetically Deterministic Methods

An alternative approach to simulating the elastic effects in the coarsening of coherent precipitates is more deterministic than the Monte Carlo method. This approach is to lower the total energy by the method of steepest energetic descent. In using this method, one stipulates the existence of some underlying physical process that will lower a system's energy as much as possible when given the opportunity. This allows one to study the kinematic path of morphological change rather than the dynamics, or rate, of coarsening in strongly elastic affected systems. The kinematics are studied by exploring the sequence of configuration states leading to local energy minima. While it is very difficult to leave local energy minima, or metastable states, at a constant temperature when using Monte Carlo methods, there are many means available to perturb a system out of a metastable state when using more deterministic methods. This kinematic information can then be used to better understand microstructural evolution by showing how the elastic driving force affects the morphology and distribution of precipitates during coarsening.

III. Analytic Model

III.A The elastic energy

The elastic contribution to the free energy of a distribution of coherent inclusions can be written in the form [42]

$$\Delta F^{el} = \Delta F^{o} + \Delta F^{c} \tag{1}$$

where ΔF^{o} is a *self-energy* which depends only on the volume of the inclusion phase, and ΔF^{c} is a *configurational energy* that depends on its spatial configuration. The configuration of the inclusion phase is described by the function, $\theta(\mathbf{r})$, which is equal to unity when the position vector, $\mathbf{r}$, falls within the inclusion phase, and is zero otherwise. Assuming linear elasticity, and using the method of Fourier transforms to evaluate the elastic field of the inclusion phase, the configurational energy is given by the integral

$$\Delta F^{c} = \frac{1}{2}\int_{\mathbf{k}} B'(\mathbf{n})\, |\theta(\mathbf{k})|^2 \frac{d^3\mathbf{k}}{(2\pi)^3} \tag{2}$$

where $\mathbf{n} = \mathbf{k}/|\mathbf{k}|$ is a unit vector in the direction of the wave vector $\mathbf{k}$, $\theta(\mathbf{k})$ is the Fourier transform of the shape function, $\theta(\mathbf{r})$,

$$\theta(\mathbf{k}) = \int_V \theta(\mathbf{r}) e^{-i\mathbf{k}\cdot\mathbf{r}} \, d^3\mathbf{r} \tag{3}$$

and $B'(\mathbf{n})$ is the *elastic relaxation function*, whose value depends on the elastic constants of the medium and on the stress-free strain, $\boldsymbol{\varepsilon}^o$, of the inclusion with respect to the matrix. The integration is taken to exclude the origin, $\mathbf{k} = \mathbf{0}$, since the contribution from the origin is included in the self-energy term.

In the case we shall study here the system has cubic symmetry and the inclusion differs from the matrix by a simple volume expansion or contraction. Then $\boldsymbol{\varepsilon}^o = \varepsilon_o \delta$, and $B'(\mathbf{n})$ is well approximated by the algebraic expression [41]

$$B'(\mathbf{n}) = -\frac{2\beta^2 \Delta \varepsilon_o^2}{c_{11}(2c_{11} - \Delta)} \left\{ 2\gamma_1(\mathbf{n}) + \frac{27\beta\Delta^2}{(2c_{11} - \Delta)(3c_{11} - 2\Delta)} \gamma_2(\mathbf{n}) \right\} \tag{4}$$

where c_{11}, c_{12}, and c_{44} are the cubic elastic constants, $\beta = c_{11} + 2c_{12}$ is the bulk modulus, and $\Delta = c_{11} - c_{12} - 2c_{44}$ is the elastic anisotropy factor. The geometric functions, $\gamma_1(\mathbf{n})$ and $\gamma_2(\mathbf{n})$ are the cubic harmonics:

$$\gamma_1(\mathbf{n}) = n_x^2\, n_y^2 + n_y^2\, n_z^2 + n_z^2\, n_x^2 \tag{5}$$

$$\gamma_2(\mathbf{n}) = n_x^2\, n_y^2\, n_z^2 \tag{6}$$

To re-cast equation (2) into the two-dimensional form that is needed for the present work, we assume that the transformation strain is areal,

$$\boldsymbol{\varepsilon}^o = \varepsilon_o \boldsymbol{\delta}_2 \tag{7}$$

where $\boldsymbol{\delta}_2$ is the unit vector in two dimensions, $(\boldsymbol{\delta}_2)_{ij} = \delta_{ix}\delta_{jx} + \delta_{iy}\delta_{jy}$, and the system is in plane strain in the (xy)-plane, which is perpendicular to one of the cubic axes. Then

$$B'(\mathbf{n}) = -\frac{4\beta^2\Delta\varepsilon_o^2}{c_{11}(2c_{11}-\Delta)}\,\gamma_1'(\mathbf{n}) \tag{8}$$

where $\gamma_1' = n_x^2\, n_y^2$. The position vector, $\mathbf{r}$, and the wave vector, $\mathbf{k}$, reduce to two-dimensional vectors in the plane, and the Fourier integral (3) is an integral over the plane. Using equation (8) in equation (2), the configurational energy is

$$\Delta F^c = \frac{1}{2}\int_{\mathbf{k}} B'(\mathbf{n})\ |\theta(\mathbf{k})|^2 \frac{d^3\mathbf{k}}{(2\pi)^3}$$

$$= 4E^* A_p I_p[\theta(\mathbf{r})] \tag{9}$$

where

$$E^* = -\frac{\beta^2 \Delta \varepsilon_0^2}{2c_{11}(2c_{11} - \Delta)} \tag{10}$$

is a material constant and convenient measure of elastic interaction energy [41], A_p is the cross-sectional area of the inclusion phase in the plane, and

$$I_p[\theta(\mathbf{r})] = \frac{1}{A_p}\int_{\mathbf{k}} \gamma_1'(\mathbf{n})|\theta(\mathbf{k})|^2 \frac{d^2\mathbf{k}}{(2\pi)^2} \tag{11}$$

is a dimensionless function whose value depends only on the configuration of the inclusion phase in the plane. Note that if $\Delta < 0$, E^* is positive; minimizing I_p also minimizes the energy. We limit this discussion to this case.

III.B The surface energy

The total configurational energy of the inclusion distribution is the sum of its elastic and interfacial energies. The surface energy of the distribution, per unit length perpendicular to the plane, can be conveniently written

$$\Delta F^s = \sigma \sqrt{A_p} L_p \tag{12}$$

where σ is the surface tension (assumed isotropic), and $L_p = L_p[\theta(\mathbf{r})]$ is the dimensionless, or normalized, line length of the inclusion. The function $L_p[\theta(\mathbf{r})]$ depends only on the shape of the inclusion phase in the plane: it is independent of size.

Adding equations (9) and (12), the total configurational energy can be written, in dimensionless form,

$$\Delta f = \frac{\Delta F^c + \Delta F^s}{4E^* A_p} = I_p[\theta(\mathbf{r})] + \frac{\sigma}{4E^* \sqrt{A_p}} L_p[\theta(\mathbf{r})]$$

$$= I_p + \frac{r_o}{D} L_p = I_p + r_o{}^* L_p \tag{13}$$

where

$$r_o = \frac{\sigma}{4E^*} \tag{14}$$

is an effective length that measures the relative contribution of the surface and elastic effects, $D = \sqrt{A_p}$ is a length that measures the size of the inclusion phase, and $r_o^* = r_o/D$. It follows that the relative energy of a particular configuration of the inclusion is determined by its shape and by its size relative to the dimensionless characteristic length, r_o, that fixes the ratio between the interfacial and elastic contributions to the energy.

IV. Equilibrium Shapes in Two Dimensions

In previous work [41] it was shown that a homogeneous, dilational inclusion in a cubic matrix with negative elastic anisotropy should undergo a monotonic shape transformation from a sphere to a cube to a doublet of parallel plates, to an octet of small cubes, and, finally, to a thin plate as its effective size, $D = V^{1/3}$, increases with respect to a characteristic length r_o. The corresponding two-dimensional sequence would be from a circle to a square to a doublet of parallel rectangles to a quartet of small squares, and finally to a thin rectangular plate.

To compare the energies of the various two-dimensional figures we need to evaluate the geometric functions, I_p and L_p. For a circle, $\theta(\mathbf{k})$ is isotropic. Hence I_c, the value of I_p for a circle, is just the average value of $\gamma'(\mathbf{n}) = n_x^2 n_y^2$ over the unit sphere:

$$I_c = \langle n_x^2 n_y^2 \rangle = \langle (\cos^2\theta)\ (\sin^2\theta) \rangle = 0.125 \tag{15}$$

For a square of edge length D = 2a, the shape function, $\theta_s(\mathbf{k})$ is

$$\theta s(\mathbf{k}) = \theta_s(h,k) = (2a)^2 \left[\frac{\sin(2\pi h)}{2\pi h}\right]\left[\frac{\sin(2\pi k)}{2\pi k}\right] \tag{16}$$

where the variables (h,k) are determined by the identities $k_x a = 2\pi h$, and $k_y a = 2\pi k$. The geometric integral I_s is

$$I_s = \frac{4}{(2a)^4} \iint \frac{h^2 k^2}{(h^2+k^2)^2} |\theta_s(\mathbf{k})|^2 \, dh dk = 0.1103 \tag{17}$$

Similar reasoning yields geometric integrals for rectangles of edge lengths, b and $c = A_p/b$. The values are plotted as a function the long edge length, b (measured in units of $\sqrt{A_p}$), in Fig. 1.

A doublet inclusion is formed by the decomposition of a square of edge length (2a) into parallel rectangles, with dimensions 2a x a, that are separated by the distance, u. The energy is minimized if the separation is in the [010] direction. The shape function, $\theta_d(\mathbf{k}) = \theta_d(h,k)$, is

$$\theta_d(h,k) = 4a^2 \left[\frac{\sin(2\pi h)}{2\pi h}\right]\left[\frac{\sin(\pi k)}{\pi k}\right]\cos[\pi k(1+\xi_d)] \tag{18}$$

where $\xi_d = u/a$. A quartet inclusion contains squares of edge length, a, that are separated by the distance u in the <100> directions. The shape function is

$$\theta_q(h,k) = 4a^2 \left[\frac{\sin(\pi h)}{\pi h}\right]\left[\frac{\sin(\pi k)}{\pi k}\right]\cos[\pi h(1+\xi_q)]\cos[\pi k(1+\xi_q)] \tag{19}$$

The integrals I_d and I_q are functions of the dimensionless separation, ξ. The function ΔF^c is plotted as a function of separation in Fig. 2. The elastic energy is minimum at the separation $\xi_d = 1.20$ for doublets and $\xi_q = 0.54$ for quartets. The values of the geometric integrals at these separations are

$$I_d(\xi_d = 1.20) = 0.0882 \tag{20}$$

$$I_q(\xi_q = 0.54) = 0.0863 \tag{21}$$

The functions, L_p, for the circle, square, rectangles, doublet and quartet are easily found by dividing the perimeter by $D = \sqrt{A_p}$. The total configurational energies are, then,

$$\Delta f(\text{circle}) = 0.1250 + 2r_o^*\sqrt{\pi} \tag{22}$$

$$\Delta f(\text{square}) = 0.1103 + 4r_o^* \tag{23}$$

$$\Delta f(\text{doublet}) = 0.0882 + 6r_o^* \tag{24}$$

$$\Delta f(\text{quartet}) = 0.0863 + 8r_o^* \tag{25}$$

$$\Delta f(\text{rectangle}) = I_p(b) + 2(b + b^{-1})r_o^* \tag{26}$$

where the values of $I_p(b)$ are given in figure 1.

Comparing these values, the circle has minimum energy when $D < 7.7r_o$, the square is preferred when $7.7r_o < D < 22.6r_o$, the doublet is preferred when $22.6r_o < D < 263r_o$, and the quartet is preferred for larger values of D. The results resemble those calculated for the three-dimensional transition from sphere to cube to octet [41], with the difference that the octet is a likely configuration in three dimensions, while the doublet to quartet transition is only favored in two dimensions when the particle size is very large. If the square to doublet transition is somehow suppressed, then the square to quartet transition is preferred when the size, D, exceeds $41.7r_o$.

However, the similarity between the two- and three-dimensional cases that is suggested by equations (22)-(26) is somewhat deceptive. The reason is that the rectangular plate has a relatively low surface energy in two dimensions, and is preferred energetically at sizes even smaller than that at which the circle transforms to a square. The rectangle that forms initially, at $D = 6.8r_o$, has edge lengths, b and c, such that its aspect ratio, $\kappa = b/c$, is 2.25. As D increases further, the equilibrium rectangle monotonically increases in aspect

ratio, steadily decreasing its elastic energy. To construct a two-dimensional simulation of the three-dimensional morphological sequence it is useful to suppress the natural tendency toward rectangular shapes in two-dimensions. This happens naturally in the finite element model described below.

V. Finite Element Model

To calculate the relative energies of distributions of inclusions we use a lumped-node finite element method in which the configuration is taken to be periodic in the plane, and each planar period is divided into a grid of square cells with edges of given length, d, that are identified by the cell center positions, $\{\mathbf{R}\}$. Each cell is either empty or filled by the inclusion phase; its occupancy is denoted by the value of the distribution function, $\zeta(\mathbf{R})$, which has the value 1 if $\mathbf{R}$ is filled and is zero if $\mathbf{R}$ is empty. The inclusion shape function, $\theta(\mathbf{r})$, is, then,

$$\theta(\mathbf{r}) = \sum_{\mathbf{R}} \eta(\mathbf{r}-\mathbf{R})\,\zeta(\mathbf{R}) \tag{27}$$

where $\eta(\mathbf{r} - \mathbf{R}) = 1$ if the position, $\mathbf{r}$, lies in the cell centered at $\mathbf{R}$ and is otherwise zero. The two-dimensional Fourier transform of $\theta(\mathbf{r})$ is

$$\theta(\mathbf{k}) = \int_A \theta(\mathbf{r})\, e^{-i\mathbf{k}\bullet\mathbf{r}}\, d^3\mathbf{r} = \eta(\mathbf{k}) \sum_{\mathbf{R}} \zeta(\mathbf{R}) e^{-i\mathbf{k}\bullet\mathbf{r}} \tag{28}$$

V.A The elastic energy

Substituting equation (28) into equation (11), the configurational integral can be written

$$I_p = \frac{1}{2A_p} \sum_{\mathbf{R},\mathbf{R}'} \omega(\mathbf{R}-\mathbf{R}')\zeta(\mathbf{R})\zeta(\mathbf{R}') \tag{29}$$

where

$$\omega(\mathbf{R}-\mathbf{R}') = 2\int_{\mathbf{k}} \gamma_1'(n)|\eta(\mathbf{k})|^2 e^{-i\mathbf{k}\bullet[\mathbf{R}-\mathbf{R}']} \frac{d^2k}{(2\pi)^2} \tag{30}$$

is the dimensionless elastic interaction between cells located at **R** and **R'**. It follows that the configurational part of the elastic energy is a simple superposition of two-body interactions between separated cells.

In order to calculate the two-body interaction function, $\omega(\mathbf{R} - \mathbf{R}')$, we assume that the distribution is periodic with period, L, along the two grid axes. Then, $\mathbf{k} = \mathbf{K} + \boldsymbol{\kappa}$, where **K** is a wave vector of the reciprocal lattice,

$$\mathbf{K} = \frac{2\pi}{d}(h_1\mathbf{e}_1 + h_2\mathbf{e}_2) \tag{31}$$

with h_i integer, and $\boldsymbol{\kappa}$ is a wave vector in the first Brillouin zone,

$$\boldsymbol{\kappa} = \frac{2\pi}{L}(n_1\mathbf{e}_1 + n_2\mathbf{e}_2) \tag{32}$$

where n_i are integers in the domain $-L/2d < n_i \leq L/2d$. The function $\omega(\mathbf{R}-\mathbf{R}')$ can be re-expressed in the form

$$\omega(\mathbf{R}-\mathbf{R}') = \frac{2}{N}\sum_{\mathbf{K}}\sum_{\boldsymbol{\kappa}}\gamma_1'(\mathbf{n})\,|\eta(\mathbf{K}+\boldsymbol{\kappa})|^2\, e^{-i\mathbf{k}\bullet[\mathbf{R}-\mathbf{R}']} \tag{33}$$

where N is the number of cells within the periodic boundary. For a square of edge length, d,

$$|\eta(\mathbf{k})|^2 = \frac{\sin^2(k_1d)}{(k_1d)^2}\frac{\sin^2(k_2d)}{(k_2d)^2} = \frac{\sin^2(\kappa_1d)}{[(K_1+\kappa_1)d]^2}\frac{\sin^2(\kappa_2d)}{[(K_2+\kappa_2)d]^2} \tag{34}$$

With these results, the configurational contribution to the dimensionless elastic energy is

$$\Delta f^c = I_p[\{\zeta(\mathbf{R})\}] = \frac{1}{2A_p}\sum_{\mathbf{R},\mathbf{R}'}\omega(\mathbf{R}-\mathbf{R}')\zeta(\mathbf{R})\zeta(\mathbf{R}') \tag{35}$$

where the function $I_p[\{\zeta(\mathbf{R})\}]$ depends on the configuration, $\{\zeta(\mathbf{R})\}$, only.

Given equations (33) and (35), the problem of computing the configurational contribution to the elastic energy of an arbitrary distribution of inclusions is reduced to the problem of determining the dimensionless two-body interaction, $\omega(\mathbf{R}-\mathbf{R}')$. While this sum is not simple to calculate, the calculation need only be done once for an array of given size. The two-body potential is independent of the values of the elastic constants and the magnitude of the transformation strain. Moreover, the simple real-space form of equation (35) makes it relatively easy to update the elastic energy for incremental changes in the inclusion configuration, and hence, to follow the change in elastic energy as the distribution evolves.

V.B The surface energy

To compute the total energy of a configuration of inclusions it is necessary to calculate the net surface energy. A particular cell of the inclusion phase contributes to the surface energy only if it lies at the surface, that is, only if it borders empty cells. To maximize contact with the analytic results presented above, we would like to adjust the interfacial interaction so that the surface tension is isotropic. This is difficult to do for a body that is made up of square cells since all boundaries except those in {10} orientations are necessarily jagged, and since the cell-cell interaction is coarse-grained with respect to the interface. As a compromise, we chose the surface interaction so that a particle in the interface interacts only with its nearest neighbors in the ⟨10⟩ and ⟨11⟩ directions, and selected the interactions, σ_{10} and σ_{11}, so that the interfacial tensions of the {10} and {11} interfaces would be the same. Accounting for the different contributions to the interfacial area from the {10} and {11} faces of a square cell, this is accomplished when

$$\frac{\sigma_{10}}{\sigma_{11}} = \frac{2\sqrt{2}-1}{2-\sqrt{2}} \approx 3.121 \tag{36}$$

in which case the tension of the {10} and {11} interfaces is

$$\sigma = \frac{\sigma_{10}+\sigma_{11}}{d} = \frac{\sigma_{10}}{d}\left[\frac{3}{2\sqrt{2}-1}\right] = \frac{\sigma_{11}}{d}\left[\frac{3}{2-\sqrt{2}}\right] \tag{37}$$

The interfacial tension for an intermediate direction is slightly larger that this number, but is nearly isotropic.

With this approximation the total interfacial energy of the configuration can be expressed in terms of the occupation of the site, **R**, and the number of empty immediate neighbors, $n_{10}(\mathbf{R})$ and $n_{11}(\mathbf{R})$, that contribute surface interactions to it:

$$\Delta F^s = \frac{\sigma d}{3} \sum_{\mathbf{R}} \zeta(\mathbf{R}) \left[(2\sqrt{2} - 1)n_{10}(\mathbf{R}) + (2-\sqrt{2})n_{11}(\mathbf{R})\right]$$

$$= \sigma\sqrt{A_p} L_p[\{\zeta(\mathbf{R})\}] \tag{38}$$

where the function, $L_p[\{\zeta(\mathbf{R})\}]$ depends on the configuration, $\{\zeta(\mathbf{R})\}$, only:

$$L_p[\{\zeta(\mathbf{R})\}] = \frac{1}{3\sqrt{N_p}} \sum_{\mathbf{R}} \zeta(\mathbf{R}) \left[(2\sqrt{2} - 1)n_{10}(\mathbf{R}) + (2-\sqrt{2})n_{11}(\mathbf{R})\right] \tag{39}$$

The total configurational contribution to the free energy is, then, given by an equation identical to equation (13):

$$\Delta f = \frac{\Delta F^c + \Delta F^s}{4E^* A_p} = I_p[\{\zeta(R)\}] + \frac{r_o}{D} L_p[\{\zeta(R)\}] \tag{40}$$

where I_p and L_p are the discrete sums over the configuration defined in equations (35) and (39), respectively.

VI. Shape Transitions in Computer Simulation

VI.A Procedure

The computer simulation experiments reported here were primarily intended to identify morphological instabilities in the inclusion phase and examine the metastable equilibrium configurations to which the unstable shape might evolve. A shape is unstable with respect to reconfiguration when there is an infinitesimal redistribution of the inclusion phase that lowers the free energy. In the present case, the elementary (infinitesimal) redistribution is a change in the location of a single cell of the inclusion phase, and the shape is unstable when there is a change in location that decreases the configurational energy.

A morphological instability initiates an evolution that can only terminate in a configuration that is at least metastable. Both the rate and path of evolution depend on the specific mechanisms that are available, including diffusion and nucleation of new particles. The general solution of diffusional coarsening would require an elaborate computational effort that is beyond the scope of this work. The present investigation is limited to a kinematic study of evolution along the "minimum energy path", the path along which the system would evolve if each elementary step were chosen to minimize the instantaneous value of the free energy. The evolution ceases when the configuration reaches a metastable state in which it is impossible to decrease the free energy by relocating a single cell.

In the computer simulation the inclusion phase fills a subset of square cells in a periodic array. The dimensionless elastic interaction function, $\omega(\mathbf{R}-\mathbf{R}')$, is a property of the array only, and is calculated from equation (33). The physical parameter that governs the configurational energy of the inclusion distribution is the dimensionless length, r_0^*, which determines the configurational energy according to equation (40).

It is unnecessary to compute the configurational energy for every configuration; we require only the configurational part of the dimensionless chemical potential

$$\mu^c(\mathbf{R}) = \frac{\delta(\Delta f)}{\delta\zeta(\mathbf{R})} \tag{41}$$

which gives the change in energy on inserting a particle at position, $\mathbf{R}$. The maximum of $\mu^c(\mathbf{R})$ among the filled cells determines the inclusion site, $\mathbf{R}_i$, whose removal would be most favorable. Then the minimum value of $\mu^c(\mathbf{R})$ among the unfilled sites (calculated after emptying $\mathbf{R}_i$) determines the site, $\mathbf{R}_i'$, where the material at $\mathbf{R}_i$ can be most favorably repositioned. The associated change in dimensionless energy is

$$\Delta f = \mu^c(\mathbf{R}_i') - \mu^c(\mathbf{R}_i) \tag{42}$$

and the configuration is unstable if $\mu^c(\mathbf{R}_i') < \mu^c(\mathbf{R}_i)$, metastable if $\mu^c(\mathbf{R}_i') > \mu^c(\mathbf{R}_i)$. Since $\mu^c(\mathbf{R})$ is linear in the distribution, $\{\zeta(\mathbf{R})\}$, the pertinent values of $\mu^c(\mathbf{R})$ can be carried in the computer in a table that is easily updated as the system evolves.

We have used this procedure to conduct two types of simulations. The first, which is the principle focus of this paper, studies the evolution of an initially circular inclusion. Given an approximate sphere of elementary cells, we decrease r_0* (increase D) until the configuration becomes unstable, then follow its evolution along the minimum energy path until it finds a new configuration. Each time a new, metastable configuration is reached we decrement r_0* to destabilize it again, thus following the evolution of shape during coarsening. In the second type of simulation we model the evolution of an initial distribution of small inclusions by setting the value of r_0* (that is, we set the ratio of surface and elastic effects along with the areal fraction of inclusion phase) and let the distribution evolve along the minimum energy path until a metastable state is reached. In this way we study the character of the first metastable state as a function of r_0*. The results of these simulations are described in turn.

VI.B Evolution of an initially circular inclusion

To describe the results of the simulation experiments that studied the evolution of a circular configuration it is consistent to take r_0 as fixed, so that D increases. Since the area fraction of inclusion cells within a period of the simulation remains constant as D increases, the periodic array coarsens at constant volume fraction of inclusion phase.

VI.B.i Circle to square

The evolution from circle to square is illustrated in Fig. 3. In the simulation shown, 1257 particles were placed in a 100x100 array in a nearly circular configuration with radius of about 20 grid cells (Fig. 3a). The most circular configuration is always unstable. The minimum energy path converts it into the near-circular figure shown in Fig. 3b, which is flattened to have only (11) and (10) faces. This behavior is a consequence of the surface tension, which is not quite isotropic and favors (11) and (10) faces.

As D is increased the near-circle remains stable until $D \cong 4r_0$, at which point it becomes unstable with respect to evolution into a square, as shown in Fig. 3c. The square is achieved by moving material from the (10) faces of the circle onto its (11) faces, shrinking the latter until only (10) faces remain. The transition from circle to square is so nearly monotonic that the transition occurs at very close to the equilibrium value of D. The transition point is, in fact, below the equilibrium value for the circle-square transition that was

calculated from equation (23) ($4r_0$ vs. $7.7r_0$). This reflects the slight anisotropy in the surface tension, which creates a preference for the square.

Note that the true equilibrium shape identified in Section 3, a rectangle with aspect ratio 2.25, does not appear. This reflects the fact that if the circle were to evolve into a rectangle it would pass through intermediate configurations that have higher energy than the square. Although the circle becomes metastable with respect to a suitable rectangle before it is metastable with respect to a square, its first *instability* leads to the square.

VI.B.ii Square to doublet

Once a square has formed from the circle, it remains stable with respect to spontaneous changes in its shape until the particle size reaches the value, $D = 27r_o$, which is significantly larger than the value, $D = 22.6r_o$, at which it would transform to a doublet particle at equilibrium. Its subsequent behavior depends on the instability mechanisms that are allowed. The reason lies in the shape of the elastic interaction, which has the consequence that the cell with the highest elastic energy in a square inclusion is located at its center; essentially, the elastic interaction is repulsive along <11>, and tries to drive the inclusion apart. At the same time, the empty site at which an inclusion would have the least elastic energy is located within the matrix at some distance outside the square in the <10> direction. Since the elastic term dominates the chemical potential at $D = 27r_o$, the most favorable reconfiguration is the dissolution of a cell at the center of the square with the nucleation of a new inclusion particle in the matrix.

This process is illustrated in Fig. 4, which shows the hollowing of the square accompanied by the formation of a thin plate that is separated from the square and spreads in the <10> direction. As D increases the separated plate extends and the square gradually hollows into a doublet, leading eventually to the metastable configuration shown in Fig. 4c, which is reached at $D = 43r_o$. This doublet-plus-plate configuration is metastable with respect to further decomposition until $D > 65r_o$, at which point the configuration splits further to form a number of thin, separated plates.

Since the nucleation of new inclusion particles in the matrix may be kinetically difficult, we explored the evolution of a system in which this step is disallowed. The results

are illustrated in Fig. 5. The precipitate again begins to split by hollowing at its center when $D > 27r_0$. However, the hollowing is more gradual and is not completed until $D \cong 65r_0$. At larger sizes the split plates split further to create a stacking of thin, separated plates. We note that the separation of the plates in the doublet, ξ, is below the equilibrium value found in section 3. In this model the separation of the plates in the doublet can only be accomplished by adsorbing inclusion cells on the outside lateral surfaces of the plates. These adsorbed cells have relatively high energy, and the separation of the plates ceases when the driving force for separation falls below the value required to create them.

The mechanism shown in Fig. 5 still initiates through what is essentially a nucleation reaction; the nucleation of matrix phase in the interior of the inclusion. Since this process may also be difficult, a further simulation was done in which matrix-phase nucleation was also disallowed; only surface perturbations were permitted. In this case the square shape remains stable to arbitrarily large values of D. To trigger instability it was necessary to introduce an artificial perturbation of the surface. Fig. 6 illustrates the effect of a notch caused by the elimination of one cell in the center of the square surface. The square remains stable in the presence of this defect until $D > 100r_0$, at which point the square becomes unstable and the defect is pulled into the particle center like a migrating void. Once the particle reaches the center, the square splits just as if the empty cell had nucleated in its center. This result re-emphasizes the striking tendency of square inclusions to split from the inside out, which is a straightforward consequence of the strong maximum of the elastic energy at the inclusion center.

VI.B.iii Square to quartet

Symmetric quartets of the type treated in the analytic calculation were never formed by the natural instabilities of the square or doublet. The square splits to a doublet, including side plates if they are allowed. The doublet then splits into rectangles. This behavior is not surprising, since the rectangle is the energetically preferred figure. However, we were able to stimulate the formation of a quartet by artificially suppressing splitting of the square until its size had become large. When the square is maintained until $D > 150r_0$ before being allowed to split it hollows in the form of a cross, as shown in Fig. 7, and splits into four rectangles that approximate a quartet, with pairs of particles separated in the [10] and [01] directions. However, the quartet is unstable. The interparticle separation increases preferentially along one of the <10> directions to achieve the metastable state shown in Fig. 7, which is, effectively, a doublet of split rectangles. At $D > 225r_0$ the square initially splits into a true quartet of squares, but this is an unstable intermediate configuration that immediately splits further into a stacking of separated plates.

VI.C Evolution of a random distribution of inclusions

The computer code is also capable of simulating the evolution of an initially random distribution of inclusion particles. In this case the dimensionless length, r_0*, is a fixed parameter; r_0 is set by the elastic properties of the medium, and D is fixed by the areal fraction of the particles. Given r_0*, and assuming evolution along the minimum energy path, an initially random distribution of inclusions evolves to a metastable configuration that depends on r_0*.

Fig. 8 illustrates the metastable configurations that were reached from the same initial configuration (Fig. 8a) at three values of r_0*. When the elastic contribution is small, $r_0 * \approx 1$, the system evolves to a configuration like that shown in Fig. 8b, which contains clusters of particles that have square or rectangular shape. Since circles cannot be made of small clusters of square cells, the square and rectangular shapes are the low-energy configurations. The cluster particles are themselves distributed in a more or less random way through the matrix; since the elastic contribution is relatively small the particles do not interact strongly with one another.

Fig. 8c shows the metastable configuration that is derived from the same starting point when $r_0 * = 0.05$. The smaller value of r_0* corresponds to a much stronger elastic contribution, and this is reflected in the configuration. The particles cluster into elongated rectangles, squares and doublets whose shapes and positions are evidently correlated to one another by the elastic interaction. Fig. 8c resembles the coarsened microstructures of Ni-Al alloys reported by Miyazaki, et al. [6]. Note, however, that the doublet particles that ap-

pear here result from the association of neighboring particles rather than the splitting of particles of larger size.

Fig. 8d shows the metastable configuration that is obtained in the extreme case $r_o^* = 0$, that is, the elastic interaction is wholly dominant. In this case the particles coarsen immediately into thin rectangles that align with one another.

VII. Discussion

VII.A Results of the model

The simulations reported above reproduce a number of phenomena that have been observed during the coarsening of coherent, cubic precipitates in anisotropic media [1-8]. These include morphological transitions that are the two-dimensional analogues of the sphere → cube → doublet or octet, and direct evolution to distributions that contain doublet particles.

The results also illustrate the difference between equilibrium and instability criteria for the shape transition. A circle evolves continuously into a square; hence the transition occurs at very nearly the equilibrium particle size. However, a square can only split into a doublet by hollowing itself out or by the inward growth of a surface perturbation. Hence the size at transition is much larger than the equilibrium value, and depends on the precise transformation mechanisms that are allowed. This behavior mimics that of three-dimensional precipitates [41]: spherical precipitates in Ni-Al are converted to cubes at sizes that are close to the equilibrium sizes predicted by the elastic theory, while cubes do not split until they grow much larger than the predicted equilibrium size. The discrepancy between the equilibrium and actual transition sizes was also noted by Johnson, Voorhees, and coworkers[28-29] who have used rather different models to study coarsening.

Perhaps the most striking feature of the computer simulation is the tendency of the square particle to split by hollowing its center. Even when the splitting was compelled to initiate from the particle surface, the incipient split was immediately drawn into the center. This reflects the fact that the elastic energy is greatest at the center of the square. A similar result holds in three dimensions; the elastic energy is greatest at the center of a cube and, if it could, the cube would split from the inside. Despite the occasional observation of hollow cross-sections of cubes in Ni-Al [6,8], this probably does not happen in three dimensions. However, splitting that starts from a perturbation on the surface of a cube experiences an elastic driving force that makes it grow rapidly toward the center, presumably in the form of tunnels that lead to the hollow cross-sections that have been seen.

Note, however, that the computer simulations reveal two independent sources for doublet particle configurations: they can be created by splitting a larger cube, or they can form through the association of separate particles during coarsening. The driving force is the same in both cases: the trend to local particle configurations with relatively low elastic energy. Similarly, equilibrium transitions can be suppressed if they require intermediate configurations of higher energy; the circle transforms to a square rather than an equilibrium rectangle.

Finally, note the role of elastic anisotropy in the morphological behavior of the simulations. The model assumed negative anisotropy ($\Delta < 0$), in which case the elastic energy strongly prefers figure with (10) habits and interfaces.

VII.B Limitations of the model

In addition to its two-dimensional character, the model studied here is limited in its geometry, its treatment of the interfacial tension, and its inability to simulate the kinetics of coarsening or identify the true kinetic path.

The geometric limitations are the finite size of the elementary cell and the finite period of the grid array. The finite cell size (d) is responsible for the appearance of metastable configurations; it is impossible to simulate a truly infinitesimal reconfiguration. Since the metastable configurations do not fully satisfy the conditions of equilibrium ($\mu = \delta\Delta F/\delta\zeta(\mathbf{R})$ is not the same for all $\mathbf{R}$), the metastable configurations identified here are actually "almost metastable" configurations that will continue to coarsen at a finite, but slow rate. The finite cell size also introduces a small corner energy at the junction of (10) or (11) faces. This energy vanishes as d becomes small, and has very little effect on particles of the size studied here. The finite array size, L, introduces effects that vary with the areal fraction of inclusions $(D/L)^2$. Experimental study of the array size effect suggests that it is relatively unimportant when $D/L < 0.5$.

The surface energy of the model has the most isotropic form we have been able to devise, but still is not quite isotropic. Its anisotropy is reflected in the instability of a circle with respect to the diamond-like configuration shown in Fig. 5, which is bounded by (10) and (11) surfaces.

Finally, the model does not specifically treat the kinetics of coarsening, and only approximates the true kinetic path by the "minimum energy" path. At the present level of computational capacity it seems necessary to do this to construct a model that has the morphological complexity of the one used here. Johnson, Voorhees and co-workers [28-29] have published informative studies of coarsening in elastic media, but are forced to treat more restricted configurations. Lee [33] has presented a simulation like the one studied here in which the configuration is made to evolve by using Monte Carlo techniques to move the elementary cells. That model, which we have also studied, yields interesting results, but only evolves at a finite rate when the "effective temperature" is so high that the inclusions become relatively diffuse and their shapes ill-defined. Each of these approaches has its strengths and limitations; the search for a better understanding of coarsening may profitably exploit them all.

VIII. References

[1] A.J. Ardell, R.B. Nicholson and J.D. Eshelby, *Acta Metall.*, **14**, 1295 (1966).

[2] E. Hornbogen and M. Roth, *Z. Metallk.*, **58**, 842 (1967).

[3] H. Gleiter and E. Hornbogen, *Mat. Sci. Eng.*, **2**, 285 (1967).

[4] J.H. Westbrook, *Z. Kristallog.*, **110**, 21 (1958).

[5] M. Doi, T. Miyazaki, S. Inoue, and T.Kozakai, in *Dynamics of Ordering Processes in Condensed Matter*, S. Komura and H. Furukawa, eds., Plenum Press, New York, 287 (1988).

[6] T. Miyazaki, M. Imamura and T. Kozakai, *Mat. Sci. Eng.* **54**, 9 (1982).

[7] M. Doi, T. Miyazaki and T. Wakatsuki, *Mat. Sci. Eng.* **67**, 247 (1984).

[8] M.J. Kaufman, P.W. Voorhees, W.C. Johnson, and F.S. Biancaniello, *Metall. Trans.*, **20A**, 2171 (1989).

[9] P.W. Voorhees, *J. Stat. Phys.*, **38**, 231 (1985)

[10] I.M. Lifshitz and V.V. Slyozov, *J. Phys. Chem. Solids*, **19**, 35 (1961)

[11] C. Wagner, *Z. Electrochem.*, **65**, 581 (1961)

[12] E.M. Lifshitz and L.P. Pitaevskii, *Physical Kinetics*, Pergamon Press, New York, 432 (1981)

[13] V. Perovic, G.R. Purdy, and L.M. Brown, *Acta Metall.*, **27**, 1075 (1976).

[14] T. Miyazaki, H. Imamura, H. Mori, and T. Kozakai, *J. Mater. Sci.*, **16**, 1197 (1981).

[15] T. Miyazaki, K. Seki, M. Doi, T. Kozakai, *Mat. Sci. Eng.*, **77**, 125 (1986).

[16] T. Miyazaki and M. Doi, *Mat. Sci. Eng.*, **A110**, 175 (1989).

[17] W.C. Johnson, *Metall. Trans.*, **14A**, 2219 (1983).

[18] W.C. Johnson, *Acta Metall.*, **32**, 465 (1984).

[19] W.C. Johnson and J.W. Cahn, *Acta Metall.*, **32**, 1925 (1984).

[20] M.B. Berkenpas, W.C. Johnson, and D.E. Laughlin, *J. Mater. Res.*, **1**, 635 (1986).

[21] P.W. Voorhees and W.C. Johnson, *J. Chem. Phys.*, **84**, 5108 (1986).

[22] P.W. Voorhees, W.C. Johnson and V.J. Laraia, in *Solute-Defect Interaction Theory and Experiment*, S. Saimoto, G.R. Purdy and G.V. Kidson, eds., Pergamon Press, New York, 409 (1986).

[23] W.C. Johnson and P.W. Voorhees, *J. Appl. Phys.*, **61**, 1610 (1987).

[24] W.C. Johnson, *Metall. Trans.*, **18A**, 233 (1987).

[25] V.J. Laraia, W.C. Johnson, and P.W. Voorhees, *J. Mater. Res.*, **3**, 257 (1988).

[26] W.C. Johnson, M.B. Berkenpas, and D.E. Laughlin, *Acta Metall.*, **36**, 3149 (1988).

[27] P.W. Voorhees and W.C. Johnson, *Phys. Rev. Lett.*, **61**, 2225 (1988).

[28] W.C. Johnson, P.W. Voorhees and D.E Zupon, *Metall. Trans.*, **20A**, 1175 (1989).

[29] W.C. Johnson, T.A. Abinandanan and P.W. Voorhees, *Acta Metall. Mater.*, **38**, 1349 (1990).

[30] Y. Enomoto and K.Kawasaki, *Acta Metall.*, **37**, 1399 (1989).

[31] K. Kawasaki and E. Enomoto, *Physica*, **A150**, 463 (1988).

[32] J. Gayda and D.J. Srolovitz, *Acta Metall.*, **37**, 641 (1989).

[33] J.K. Lee, *Metall. Trans.*, **22A**, 1197 (1991).

[34] P.H. Leo and R.F. Sekerka, *Acta Metall.*, **37**, 3139 (1989).

[35] P.H. Leo, W.W. Mullins, R.F. Sekerka, and J. Vinals, *Acta Metall. Mater.*, **38**, 1573 (1990).

[36] S.H. Wen, A.G. Khachaturyan and J.W.Morris, Jr., in *Proc. Int. Symp. Modulated Struct.*, AIP, New York, p. 168 (1979).

[37] S.H. Wen, A.G. Khachaturyan and J.W.Morris, Jr., in *Proc. Int. Conf. Martensitic Trans.*, MIT, Cambridge, Mass, p. 94, (1979).

[38] S.H. Wen, A.G. Khachaturyan and J.W.Morris, Jr., *Metall. Trans.* **12A**, 581 (1981).

[39] S.H. Chen (Wen), Ph.D. Thesis, Dept. Materials Science, University of California (Berkeley), 1979 (Lawrence Berkeley Laboratory Rept. LBL-9269, June, 1979).

[40] A.G. Khachaturyan, *Theory of Structural Transformations in Solids*, Wiley, New York (1983).

[41] A.G. Khachaturyan, S.V. Semenovskaya and J.W.Morris, Jr., *Acta Metall.*, **36**, 1563 (1988).

[42] A.G. Khachaturyan and G.A. Shatalov, *Soviet Phys.-Solid State*, **11**, 118 (1969); *Soviet Phys.-JETP* **29**, 557 (1969).

[43] J.J. Weins and J.W. Cahn, in *Sintering and Related Phenomena*, G.C. Kucczynski, ed., Plenum Press, New York, 151 (1973).

[44] A.J. Ardell, *Acta Metall.*, **20**, 61 (1972).

[45] C.K.L. Davies, P. Nash and R.N. Stevens, *Acta Metall.* , **28**, 179 (1980).

[46] A.D. Brailsford and P. Wynblatt, *Acta Metall.*, **27**, 489 (1979).

[47] J.D. Gunton, in *Decomposition of Alloys: The Early Stages*, P. Haasen, V. Gerold, R. Wagner, and M.F. Ashby, eds., Peramon Press, New York, 1 (1984).

[48] C.W.J. Beenakker, *Phys. Rev.*, **A33**, 4482 (1985).

[49] M. Marder, *Phys. Rev.*, **A36**, 858 (1987).

[50] K. Kawasaki, *Physica*, **A163**, 59 (1990).

[51] T. Imaeda and K. Kawasaki, *Physica*, **A164**, 335 (1990).

[52] R.T. DeHoff, *Acta Metall. Mater.*, **39**, 2349 (1991).

[53] J.D. Eshelby, *Prog. Solid Mech.*, **2**, 89 (1961)

[54] R.G. Pahl, Jr., and J.B. Cohen, *Scripta Met.*, **18**, 397 (1984)

IX. Figures

Figure Captions

Figure 1: Values of the geometric integral, I_p, for rectangles as a function of the long edge length, b. The edge length is measured in units of $\sqrt{A_p}$.

Figure 2: The dependence of the geometric integrals on the dimensionless separation for the cases of doublets and quartets.

Figure 3: The sequence (a) - (c) displays the simulated circle → square transition.

Figure 4: The sequence (a) - (c) displays the simulated square → plate doublet transition in the case of free nucleation.

Figure 5: The sequence (a) - (c) displays the simulated square → quartet transition in the case of allowed matrix phase nucleation.

Figure 6: The sequence (a) - (c) displays the effect of surface perturbations upon a square precipitate when nucleation is not permitted.

Figure 7: The sequence (a) - (c) displays the square → quartet transition in the case of allowed matrix phase nucleation.

Figure 8: An initial random array (a) evolves to its first metastable state under the conditions of: (b) high surface to elastic energy ratio, (c) intermediate surface to elastic energy ratio, and (d) zero surface contribution.

Geometric Integrals vs. Rectangle Long Edge Length

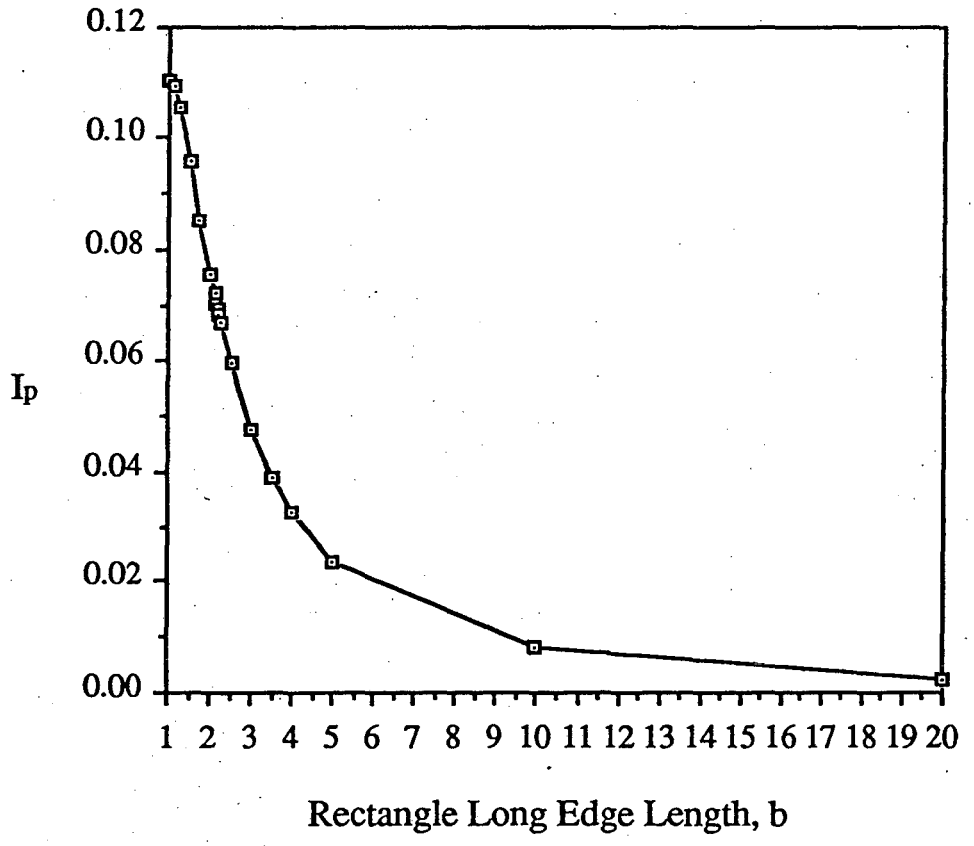

Figure 1

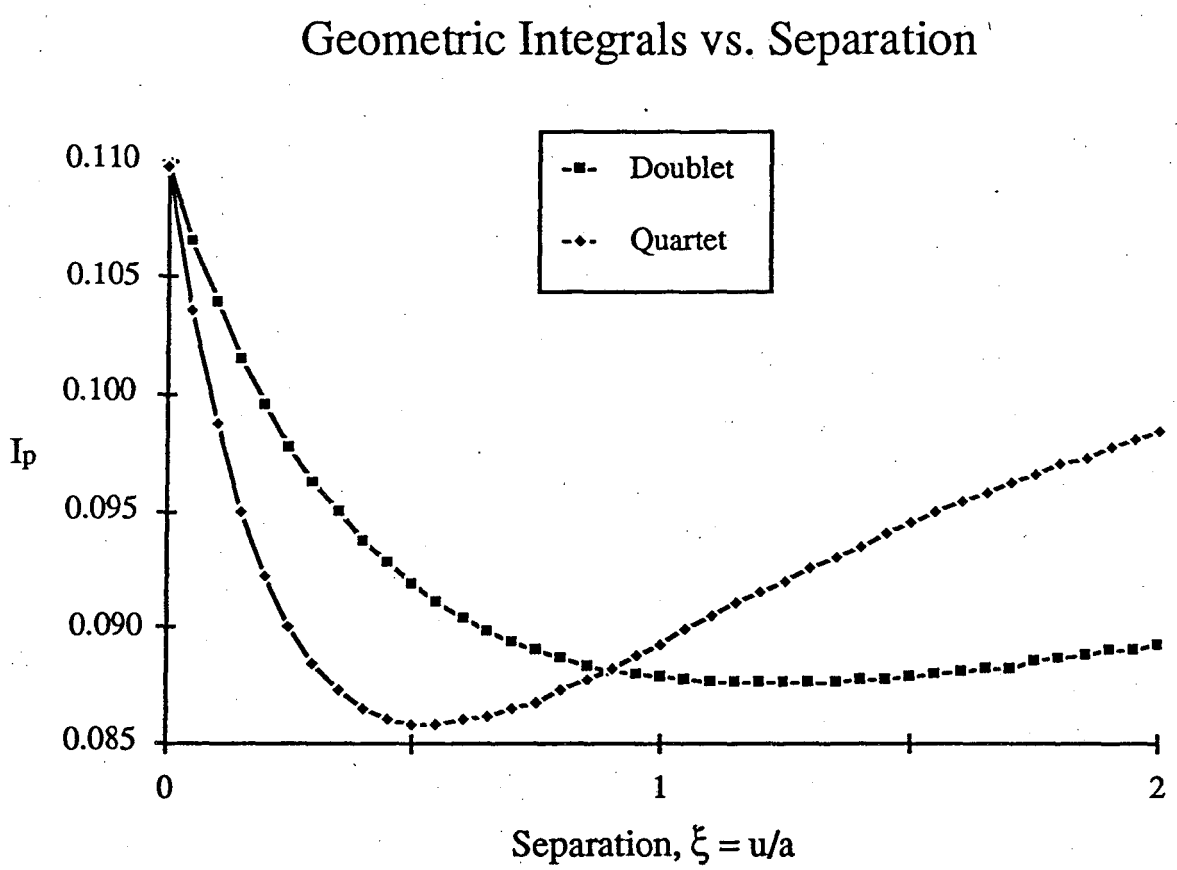
Geometric Integrals vs. Separation
Doublet
Quartet
0.110
0.105
0.100
0.095
0.090
0.085
Ip
0
1
2
Separation, ξ = u/a

Figure 2

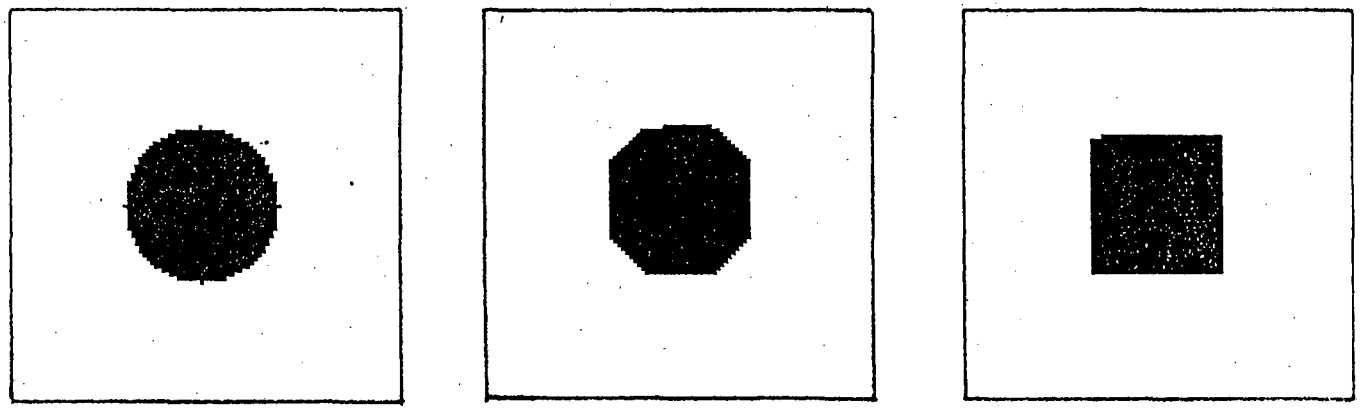

(a) (b) (c)

Figure 3

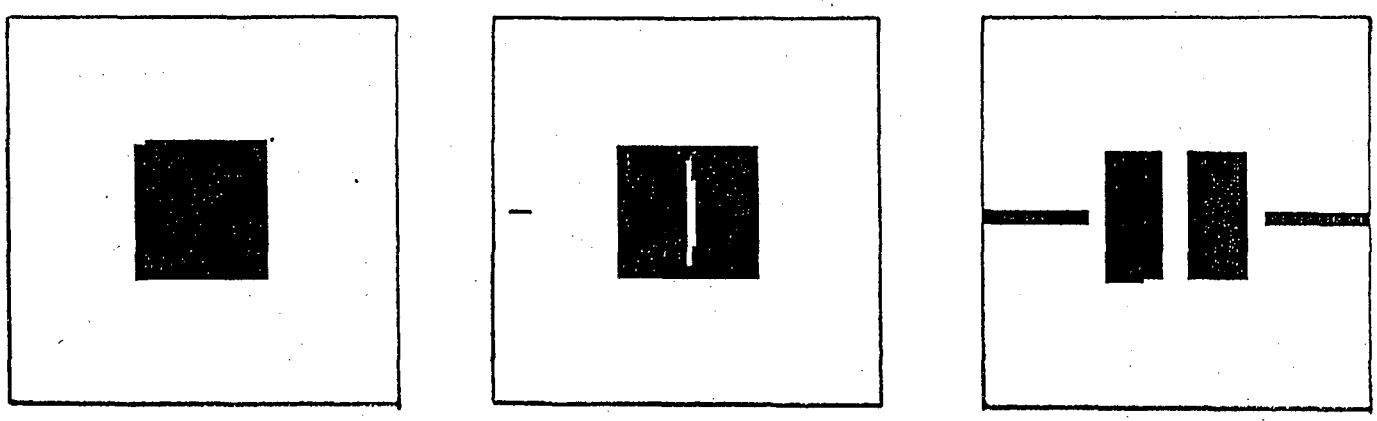

(a) (b) (c)

Figure 4

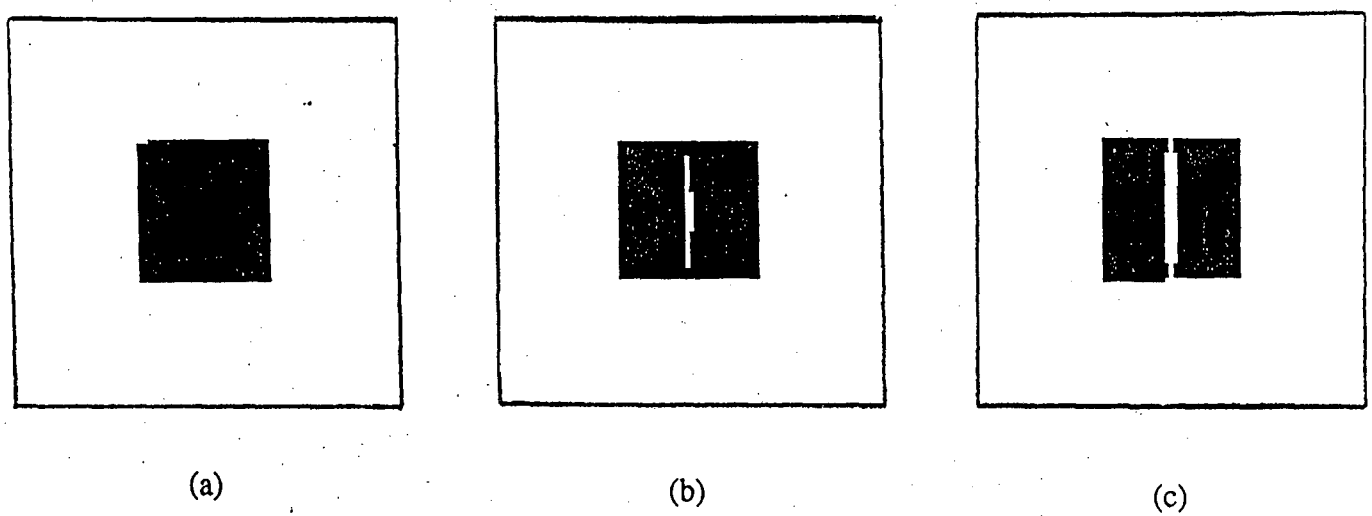

Figure 5

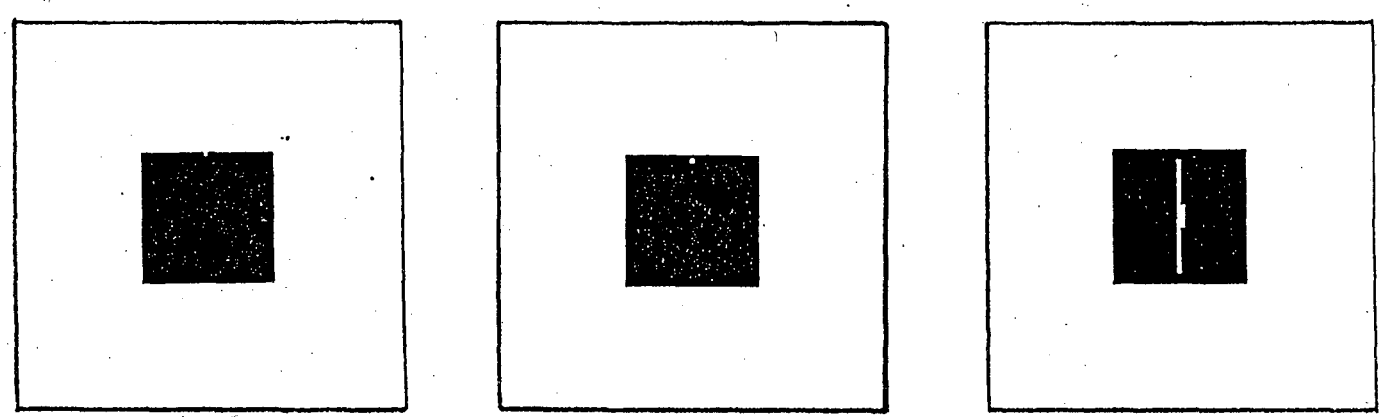

(a) (b) (c)

Figure 6

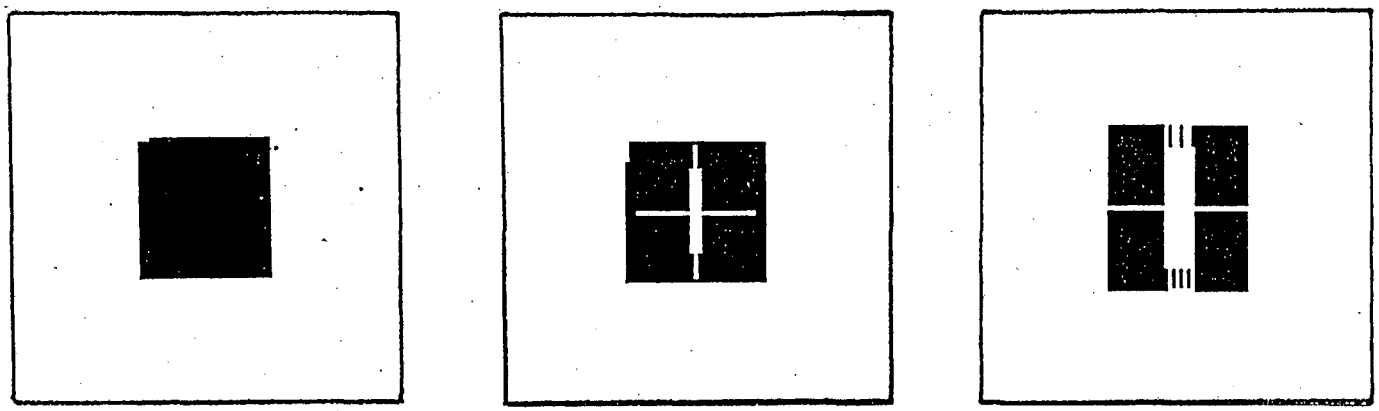

(a) (b) (c)

Figure 7

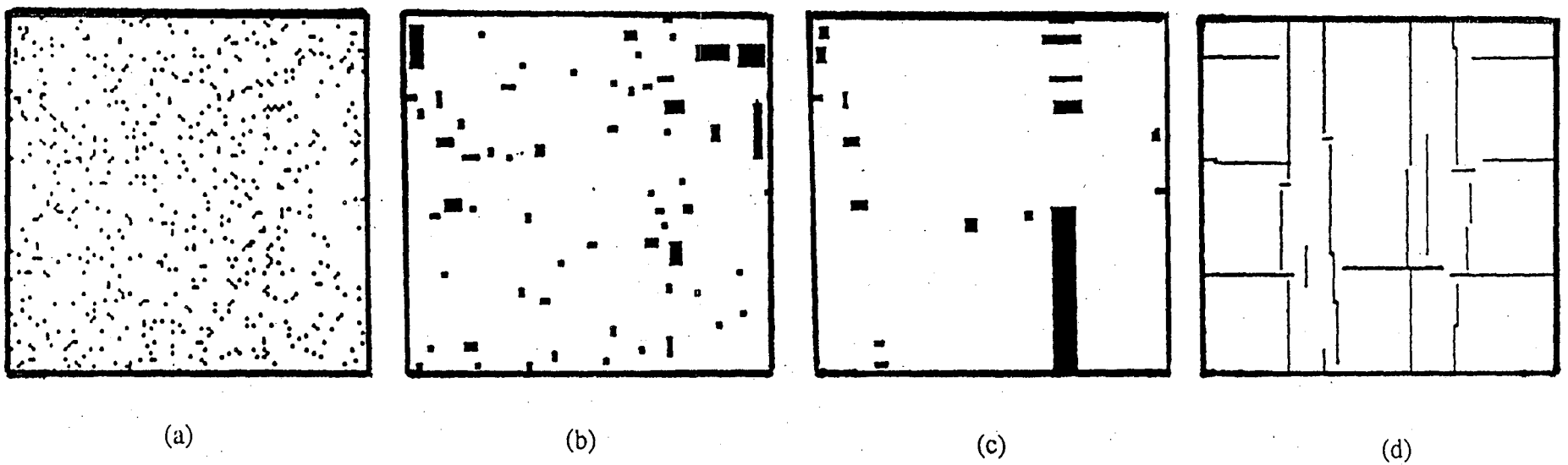

Figure 8

LAWRENCE BERKELEY LABORATORY
UNIVERSITY OF CALIFORNIA
TECHNICAL INFORMATION DEPARTMENT
BERKELEY, CALIFORNIA 94720